Hindawi Publishing Corporation
Mathematical Problems in Engineering
Volume 2013, Article ID 764812, 9 pages
http://dx.doi.org/10.1155/2013/764812

Research Article

Evaluation of Flow-Induced Dynamic Stress and Vibration of Volute Casing for a Large-Scale Double-Suction Centrifugal Pump

Fu-Jun Wang, Li-Xia Qu, Ling-Yan He, and Jiang-Yong Gao

College of Water Resources & Civil Engineering, China Agricultural University, Beijing 100083, China

Correspondence should be addressed to Fu-Jun Wang; wangfj@cau.edu.cn

Received 28 June 2013; Accepted 15 July 2013

Academic Editor: Song Cen

The transient analysis was carried out to investigate the dynamic stress and vibration of volute casing for a large double-suction centrifugal pump by using the transient fluid-structure interaction theory. The flow pulsations at flow rate ranging from 60% to 100% of the nominal flow rate (Q_d) were taken as the boundary conditions for FEM analysis of the pump volute casing structure. The results revealed that, for all operating conditions, the maximum stress located at the volute tongue region, whereas the maximum vibration displacement happened close to the shaft hole region. It was also found that the blade passing frequency and its harmonics were dominant in the variations of dynamic stress and vibration displacement. The amplitude of the dominant frequency for the maximum stress detected at 0.6 Q_d was 1.14 times that at Q_d, lower than the related difference observed for pressure fluctuations (3.23 times). This study provides an effective method to quantify the flow-induced structural dynamic characteristics for a large-scale double-suction pump. It can be used to direct the hydraulic and structural design and stable operation, as well as fatigue life prediction for large-scale pumps.

1. Introduction

Double-suction centrifugal pumps are widely employed in large-scale pumping stations. For instance, 8 large-scale double-suction centrifugal pumps with power of 7.5 MW for each are installed in the China South-to-North Water Diversion Project [1]. The effect of the complicated internal flow, together with the complicated operating conditions in engineering applications, leads to increasing concerns in operation stability, such as dynamic stress related fatigue life, vibration related noise, wear, and leakage. The problem about how to ensure pump safe and stable operation under extremely complicated operating conditions is becoming a key issue for large-scale pumping stations. An impeller of diameter 1.2 m installed in Shanxi Zuncun pumping station was found cracked after only two months of operation, without reasonable explanations so far. Such kind of problems has been pushing engineers to study more the mechanism not only in the unsteady fluid characteristics, but also in the structural dynamic characteristics including dynamic stress, vibration related issues, and also fatigue life prediction, especially in large pump units.

The fluid-structure interaction is well accepted as the principle source of vibration and noise. To some extent, the pressure fluctuations in double-suction centrifugal pumps caused by internal flow are more likely to be the primary sources of operation instability. Vast research investigations concerning issues of stability for centrifugal pumps have been conducted and reported in the open literatures. For instance, Chu et al. [2, 3] used velocity distributions determined by means of particle displacement velocimetry (PDV) to compute the pressure field within the volute of a centrifugal pump, revealing the relationship between unsteady flow structure, pressure fluctuations, and noise generation within centrifugal pumps. Toussaint [4] experimentally studied the unsteady flow in a centrifugal pump at off-design point operation and found that the unsteady pressures due to the rotor-stator interactions took place at the following characteristic frequencies: rotation frequency, blade passing frequency, and their harmonics. Lately, Yao et al. [5] carried out several

tests on double-suction centrifugal pumps. He found that the impeller rotating frequency and some lower frequencies dominated in suction chamber. The latter was adjacent to the 1/3 impeller rotating frequency at the design and higher flow rates ($Q \geqslant Q_d$). However, at partial flow rates ($Q < Q_d$), the magnitudes as well as the range of the lower frequencies became notably large. The blade passing frequency dominated in the volute, with the largest magnitude occurred at the tongue zone. In addition, the peak-peak value of pressure fluctuation increased markedly as the flow rates deviate from the designed ones and reached 4~5 times higher at the partial flow rates. Nevertheless, previous experimental research works have given us a comprehensive understanding of the mechanism of the pressure fluctuations induced by rotor-stator interaction. However, the understanding to the pressure fluctuations and dynamic stress acting on the double entry impeller with twisted and staggered blades is insufficient as yet, especially in large-scale pump units, due to the huge cost of time and resources.

Nowadays, computational fluid dynamics (CFD) analysis has been successfully used to solve the unsteady three-dimensional viscous flow in the impeller and volute casing of a centrifugal pump and obtain the unsteady pressure distribution. González et al. [6] verified the capability and reliability of CFD in capturing the internal three-dimensional unsteady flow in a double-suction centrifugal pump via URANS method, especially the rotor-stator interaction phenomena. Cong and Wang [7] and Qu et al. [8, 9] investigated the pressure fluctuations of turbulent flow within a double-suction centrifugal pump, showing that the blade passing frequency dominated the pressure fluctuations near the volute tongue at the design and large flow rate conditions. Yang [10] made great efforts on improving the simulation accuracy in centrifugal pump by adapting new subgrid-scale (SGS) models and near wall solution methods in large eddy simulation (LES). Hence, the rapid development of CFD provides strong technical support for the structural dynamic analysis. Kobayashi et al. [11] numerically predicted the static stress on pump blade, which agrees with the experimental results within −11~+6% accuracy. The accuracy might be affected by the ignored dynamic characteristic. Furthermore, with regard to the flow-induced structural dynamic characteristics, large-scale data transfer among different meshes (fluid structure) and the requirement for a huge amount of computational power have been considered as the main technical difficulties in previous numerical studies.

Overall, the above research works were mainly carried out within small-scale models. Yet, it is unclear whether the understanding of pressure pulsations acts the same as large-scale pump units. Qu et al. [12] investigated the unsteady flow within a large-scale double-suction centrifugal pump, revealing that the maximum amplitude of pressure fluctuations observed at 0.6 Q_d was almost 3.2 times of that at Q_d. Based on the solved unsteady flow field, Gao et al. [13] and He et al. [14] reported the structural dynamics characteristics of the impeller, which attracts a lot of attentions due to its complex and special status. They found that the fundamental frequency of the impeller was rotation frequency and its harmonics, with the maximum amplitude of stress and deformation at 0.6 Q_d being 2.8 times and 1.9 times of that at Q_d, but without giving more information about the pump body. Should they have similar characteristics and what is the correspondence between pressure pulsations and dynamic stress, as well as deformation, not only in terms of qualification but also in quantification? Hence, the current work aims to investigate the structural dynamics characteristics and try to quantify the flow-induced vibration and stress of pump casing in a large double-suction centrifugal pump at different operating conditions, by adapting finite element methods based on a newly developed fluid-structure coupling interface model, focusing on the overlooked pump body.

2. Mathematical Method

The pressure pulsations obtained from flow simulation using RNG k-ε model [12], regarding to the whole pump interior flow simulation, were set as the force boundary condition. Details with regard to fluid mechanics can be referred to [12]. Afterwards, the fluid-structure interaction was considered. There are two strategies for the solution of the fluid-structure interaction, namely, strongly coupling method and weakly coupling method [15]. In present study, the structural simulation was carried out based on weakly coupling method, which is also called the sequential coupled fluid-structure interaction. Accordingly, the effect of structural deformation to the flow field was neglected in such applications [15]. This method has been successfully adapted and improved in previous studies [13, 16, 17]. However, these investigations [13, 17] were only focused on pump impeller or hydraulic turbine. Reference [16] presented a fluid-structure coupling interface model. It is necessary to study the dynamic stress in pump volute casing.

Regarding the mainly technique difficulty, namely, transferring the pressure loads acting on the coupling interface of two grid systems, a newly developed fluid-structure coupling interface model [16] was adapted. Three steps were involved, namely, load output from flow field, load transfer between flow field and structure field, and load application automatically onto structure field, respectively. In order to improve the efficiency through saving searching time and storage space, the load transfer was carried out only on the coupling interface based on the local mesh information. A near-point weighted average method was adapted to the mesh matching and corresponding pressure load transfer. A related flow chart was shown in Figure 1, which outlines the mainlprocedure.

With the obtained input pressure load acting on the interface of the structure field, the structural simulation was followed. The governing equation for dynamic elastic vibration of structure is [18]

$$M_s\ddot{u}(t) + C_s\dot{u}(t) + K_s u(t) = F(t), \tag{1}$$

where M_s is a mass matrix, C_s is a damping matrix given by the Rayleigh's theory, K_s is a stiffness matrix, and $u(t)$, $\dot{u}(t)$, $\ddot{u}(t)$ represent a displacement vector, a velocity vector, and an acceleration vector, respectively, and $F(t)$ indicates the force acting on the structure, including pressure and gravity.

An implicit algorithm, Newmark time integration method [18], was adapted to solve (1), getting node

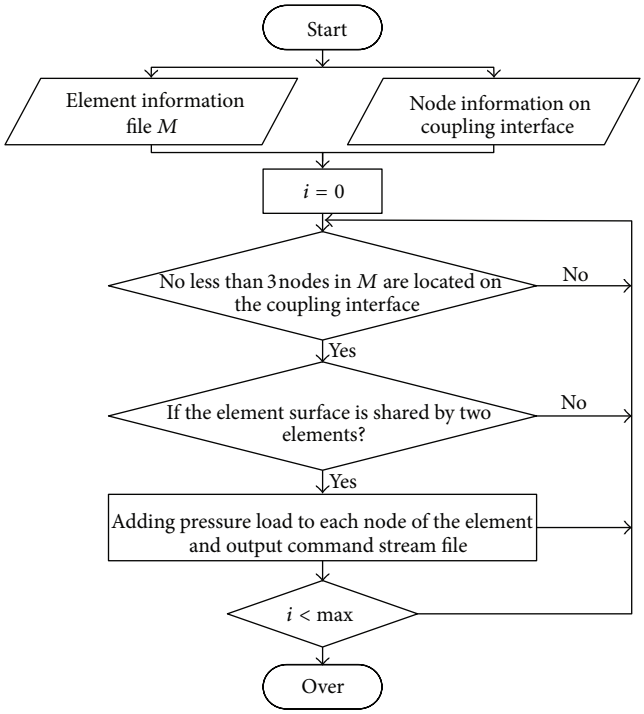

Figure 1: Flow chart of load transfer from fluid field to structure field.

displacement vectors. Then, instantaneous node stress σ can be obtained by substituting u from (1) into the following equation:

$$\sigma = DBu, \tag{2}$$

where D is elastic matrix determined by material elastic modulus and Poisson ratio and B is strain matrix based on unit shape function.

A fluid-structure coupling model developed by Yang et al. [16] was adapted to transfer the pressure loads from the internal flow field onto the structure field. More details about the adapted methods can be referred to [10, 11, 13, 15]. Moreover, our research group has carried out various experiments with small scale pumps, which have validated this method.

3. Pump Investigated and Initial Conditions

The investigated pump is a double-suction centrifugal pump, with a staggered impeller which has a V-shape cut at the exit of the blades, see Figure 2.

The main parameters are given in Table 1. The computational finite element model, together with the reference coordinate settings, is shown in Figure 3. Considering the complexity of the geometry, unstructured tetrahedral elements were adapted to discrete the computational domain, with critical regions such as the volute tongue being locally refined. The model consists of 201250 elements and 58090 nodes. The simulation was carried out under three flow conditions (0.6 Q_d, 0.8 Q_d, and 1.0 Q_d).

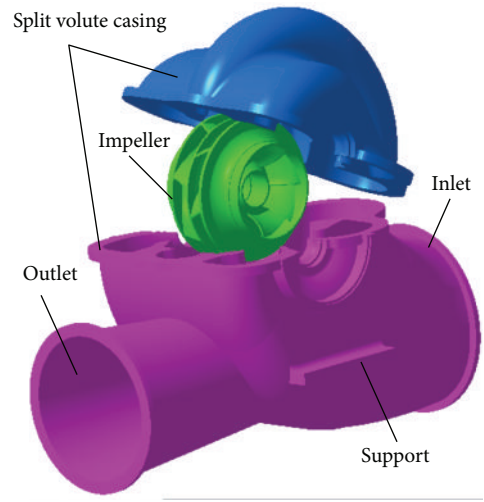

Figure 2: Pump structure.

Now that the boundary condition and initial condition were taken from the solved internal flow field by CFD, other essential settings for structural simulation are as follows.

(1) Material properties: elastic module $E = 210$ GPa, Poisson ratio $\nu = 0.3$, and density $\rho = 7800$ kg/m^3.

(2) Constraints imposed: the displacement of nodes on foundation bolt hole was set as $ux = uy = uz = 0$, while on bearing hole was $ux = uy = 0$ and $ux = 0$ on inlet and outlet flanges.

(3) Load: the fluid pressure taken from the full developed internal flow field was adapted as external dynamic force acting on pump structure. The unsteady flow simulation results for this pump could be seen in [12]. As an example, the obtained pressure fluctuations for the volute tongue are shown in Figure 4. Here, the pressure fluctuation values were presented in normalized form to allow the scaling of pressure fluctuation amplitude data with respect to size and speed, named the instantaneous pressure coefficient, which is defined as

$$C_p = \frac{\Delta P}{(\rho u_2^2/2)}, \tag{3}$$

where C_P is the pressure coefficient; ΔP is the difference between transient pressure and average pressure; u_2 is the tangential velocity of the impeller tip. Also in Figure 4, f is the rotation frequency and f_n is the blade passing frequency. The coupled interface model was introduced by Yang et al. [16] and Gao et al. [13].

(4) Integration time: 300 time steps (3 rotations) were picked out for each operating condition, with time step as 0.0016 s.

4. Results and Discussions

The dynamic stress and vibration displacement distribution on the pump were analyzed and compared at three flow

Table 1: Main parameters of the investigated pump.

Parameters	Q_d	H_d	n_d	P	D_{out}	D_{in}	D_2	Z
Value	10 m^3/s	59.2 m	375 rpm	7.5 MW	1.8 m	2.0 m	1.75 m	7

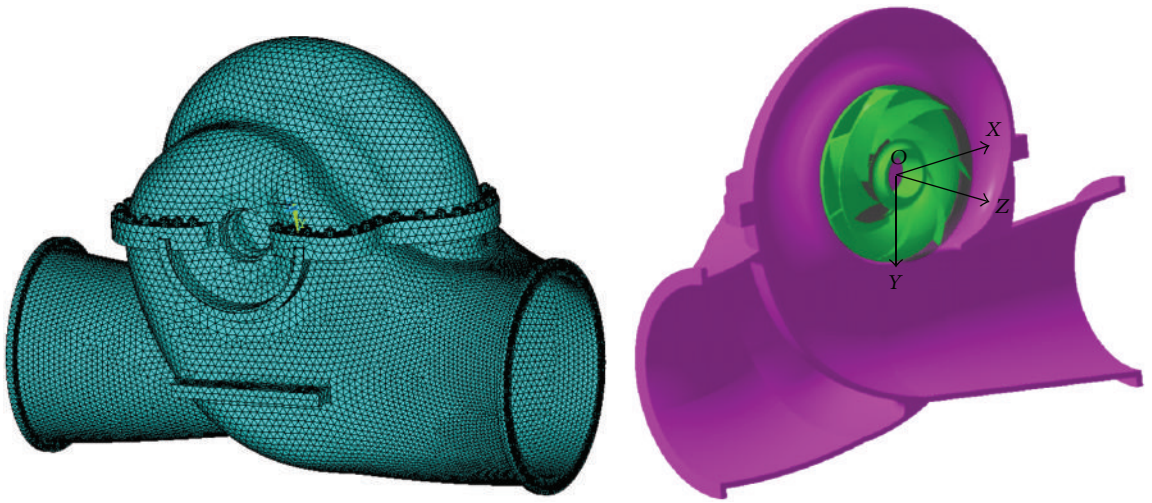

(a) Computational mesh (b) Reference frame

Figure 3: Computational mesh and reference frame.

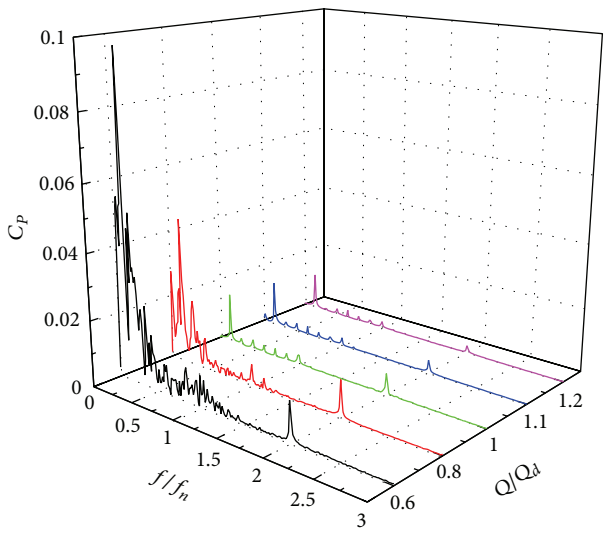

Figure 4: The pressure fluctuations at volute tongue.

conditions. The detailed analyses and discussions are as follows.

4.1. Dynamic Stress. Due to the symmetric structure of the pump body, the obtained dynamic stress distributes symmetrically at different operating conditions. In terms of time evolution, the dynamic stress behaves periodically because of the periodical interactions between the rotator and stator. Since no significant difference can be observed at different time instant at a specific given flow rate, so for the sake of clarity, only a typical instant was picked out to show the instantaneous dynamic stress distributions in Figure 5, at 0.6 Q_d and 1.0 Q_d. It can be seen that both the stress levels and distributions vary with flow rates, but the maximum values are all located close to the volute tongue, which corresponds to the maximum pressure pulsation observed in the internal flow field [12]. Moreover, at part load condition, that is, 0.6 Q_d, the stress level appears to be relatively large, see Table 2.

Table 2: Dominant frequency and corresponding amplitudes of dynamic stress at volute tongue.

Flow rate	0.6 Q_d	0.8 Q_d	1.0 Q_d
Dominant frequency (Hz)	159.9	159.9	159.9
Amplitude (MPa)	8.471	8.139	7.864

With regard to the maximum dynamic stress detected at the volute tongue (marked as N_g), a detailed spectrum analysis was carried out, see Figure 6. In Table 3, the dominant frequency and corresponding amplitudes of the dynamic stress at N_g were summarized. It can be seen, that for all considered flow rates, the dominant frequency equal to the blade passing frequency (160 Hz) and its harmonics associated with the 6th and 11th natural frequency of the pump [15] as well. However, with a decrease of flow rates from Q_d to 0.6 Q_d, the dominant frequency amplitude increased by 8% lower than the corresponding variations of the pressure pulsations obtained nearby, that is, 22.3%.

4.2. Dynamic Deformations. A periodical variation of the total vibration displacement with regard to the impeller

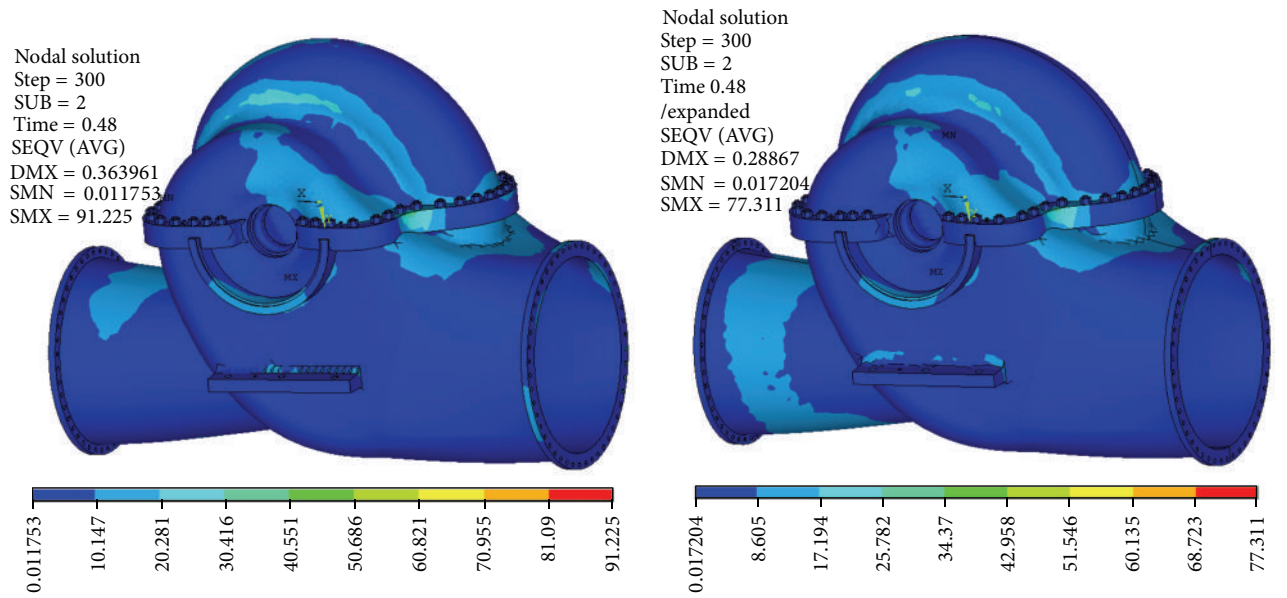

(a) 0.6 Q_d (b) 1.0 Q_d

Figure 5: Contours of stress at part load conditions.

Table 3: Dominant frequency and corresponding amplitude of vibration displacement on the pump.

Flow rates	0.6 Q_d	0.8 Q_d	1.0 Q_d
U1			
Frequency (Hz)	152.6	152.6	152.6
Amplitude (μm)	17.78	17.15	16.35
U2			
Frequency (Hz)	107.4	107.4	107.4
Amplitude (μm)	15.63	14.35	12.40
U3			
Frequency (Hz)	152.6	152.6	152.6
Amplitude (μm)	11.20	10.98	10.27
U4			
Frequency (Hz)	159.9	159.9	159.9
Amplitude (μm)	45.02	43.33	42.02
U5			
Frequency (Hz)	159.9	159.9	159.9
Amplitude (μm)	84.45	81.34	78.66
U6			
Frequency (Hz)	159.9	159.9	159.9
Amplitude (μm)	56.80	54.57	52.82

rotation was obtained for each operating condition. Hence, only four comparatively typical instants were picked out to be analyzed in the following text. The time instants were chosen at t = 0.1 T, 0.2 T, 0.8 T, and 0.9 T, where T represented the rotating time for a revolution. Figure 7 shows that the contours of vibration displacement surround the pump at four-time instants under part load condition 0.6 Q_d. Different views were set to show the location with maximum vibration displacement, with regard to different time instants. Obviously, a symmetrical distribution can be observed due to its symmetric structure. The distributions of the total vibration displacement varied with time, which indicated that the vibration displacement was associated with the rotation of impeller.

Significant high levels of vibration displacement can be mainly detected in four regions, namely, between the fourth and fifth hydraulic profiles, the sixth hydraulic profile of the volute casing close to the suction chamber wall, shaft bearing hole nearby, and the bottom of pump suction chamber close to inlet nozzle. The fourth till sixth hydraulic profile of the volute casing are within the high pressure region, experiencing strong pressure fluctuations caused by blade exit edge acting with the stationary volute casing wall, plus the shared wall with suction chamber close to the located separator can be considered as a cantilever beam. Therefore, it is reasonable to occur as comparatively large vibration displacement. As to the high levels observed around the suction part, they must be related to the structure characteristics, since the sixth and seventh natural mode shapes show significant deformation in this region [15].

4.3. Vibrations. In order to investigate the vibration status of the pump, six critical locations (Figure 8) were chosen to carry out frequency analysis. It can be seen that U1 was located on the inlet flange, U2 on the outlet flange, U3 on the top of the volute casing, U4 on the top of the suction chamber, U5 close to shaft hole, and U6 within the relative high-level region of vibration displacement.

The dominant frequency and corresponding amplitude of vibration displacement were summarized in Table 3. Each location has the same dominant frequency at various operating conditions, whereas the corresponding amplitude increased at part load conditions, that is, 8.7% at U1, 2.6%

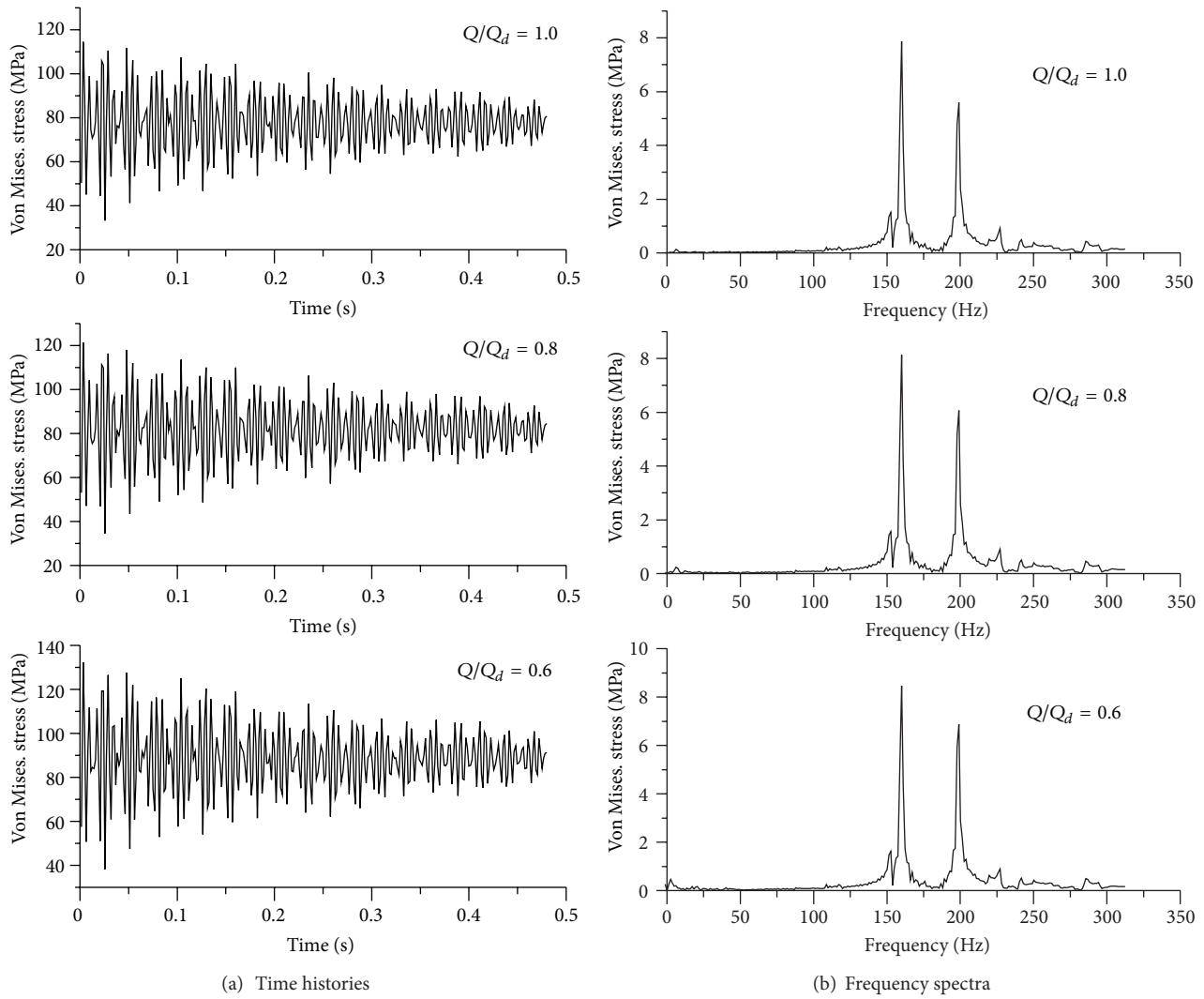

Figure 6: Dynamic stress at volute tongue.

at U2, 9.1% at U3, 7.1% at U4, 7.4% at U5, and 7.5% at U6, comparing 0.6 Q_d with Q_d. Clearly, the vibration status at the pump outlet (U2) was slightly affected by flow rate variation, whereas the top region of the volute casing (U3) appeared quite sensitive to the operating conditions. Considering the absolute values of the dominant frequency amplitudes, location U5 has the maximum level, almost 7.54 times the minimum value at U3 for 0.6 Q_d, 7.41 times for 0.8 Q_d, and 7.66 times for Q_d, respectively. As a typical location, U5, with the largest levels of vibration displacement, the related spectrum analysis was shown in Figure 9.

From the modal analysis of the pump body [15], it is known that the first, second, and sixth natural frequencies are 53.6 Hz, 110.5 Hz, and 160.29 Hz, respectively. The blade passing frequency is 87.5 Hz at nominal flow rate. The spectrum analysis, as in Figure 8, reveals that the fundamental frequency of pump vibration is blade passing frequency and its harmonics, which is also close to the pump natural frequency. However, it is of interest to note that the dominant frequency of the impeller vibration was reported to be equal to the rotation frequency and its harmonics, with the maximum amplitude at 0.6 Q_d being 2.84 times of that at Q_d [10].

The previous unsteady flow simulation indicated that the pressure fluctuations of the internal flow were actually dominated by rotation frequency and its harmonics [12]. Take the volute tongue for example, the maximum amplitude at 0.6 Q_d was 3.23 times of that at Q_d. The same trends were observed for stress on the pump body, with the maximum amplitude at 0.6 Q_d being 1.14 times of that at Q_d. Presumably, the vibration of pump body was mainly caused by the interaction between impeller and volute tongue. However, comparing the variations of pressure fluctuations with dynamic stress and deformations, it was indicating that the structure dynamic characteristics were not exactly in accordance with pressure pulsations, in terms of fluctuation strength.

We reported some experimental results for vibrations of a small-scale double-suction centrifugal pump in [19]. The numerical result for dominant frequency and its amplitude at U3 in the current study is consistent with the

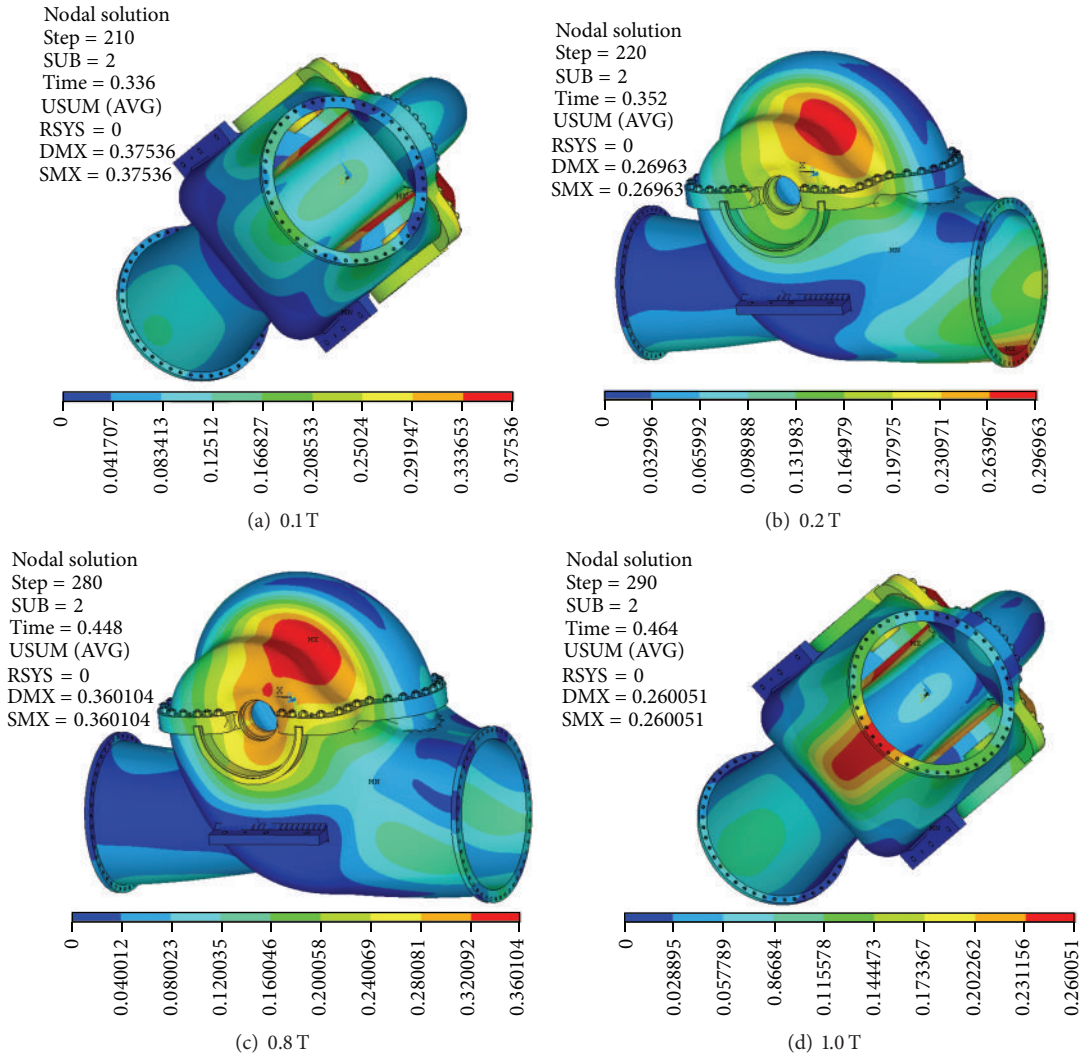

Figure 7: Contours of vibration displacements at 0.6 Q_d.

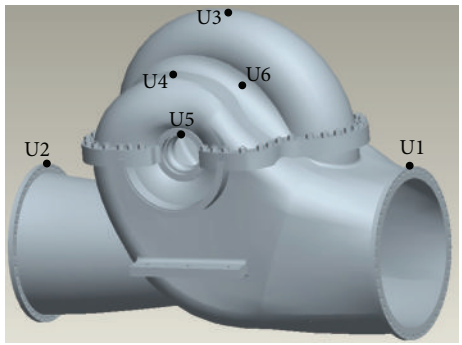

Figure 8: Positions of the data sampling point set on the outer surface of the pump.

experimental data in [19]. This demonstrates that the numerical method and the results are acceptable to reveal the dynamic behaviours of a large-scale double-suction pump body.

5. Conclusion

The flow-induced vibration for a large-scale double-suction centrifugal pump was predicted using FEM. The structural simulation was coupled with the hydrodynamic flow field through a newly developed fluid-structure coupling interface model. The adapted method was proved to be effective and accurate in quantifying the flow-induced dynamic structural characteristics. The dynamic stress and vibration were investigated under three flow conditions. The results indicate the following.

(1) The maximum dynamic stress occurred at the volute tongue region, whereas the maximum vibration displacement appeared at different positions within each rotation period. Both the dynamic stress and the vibration were dominated by the blade frequency and its harmonics, with the corresponding amplitudes increasing with the drop of flow rates. The vibration of the pump body was believed to be caused by the interactions between impeller and volute tongue.

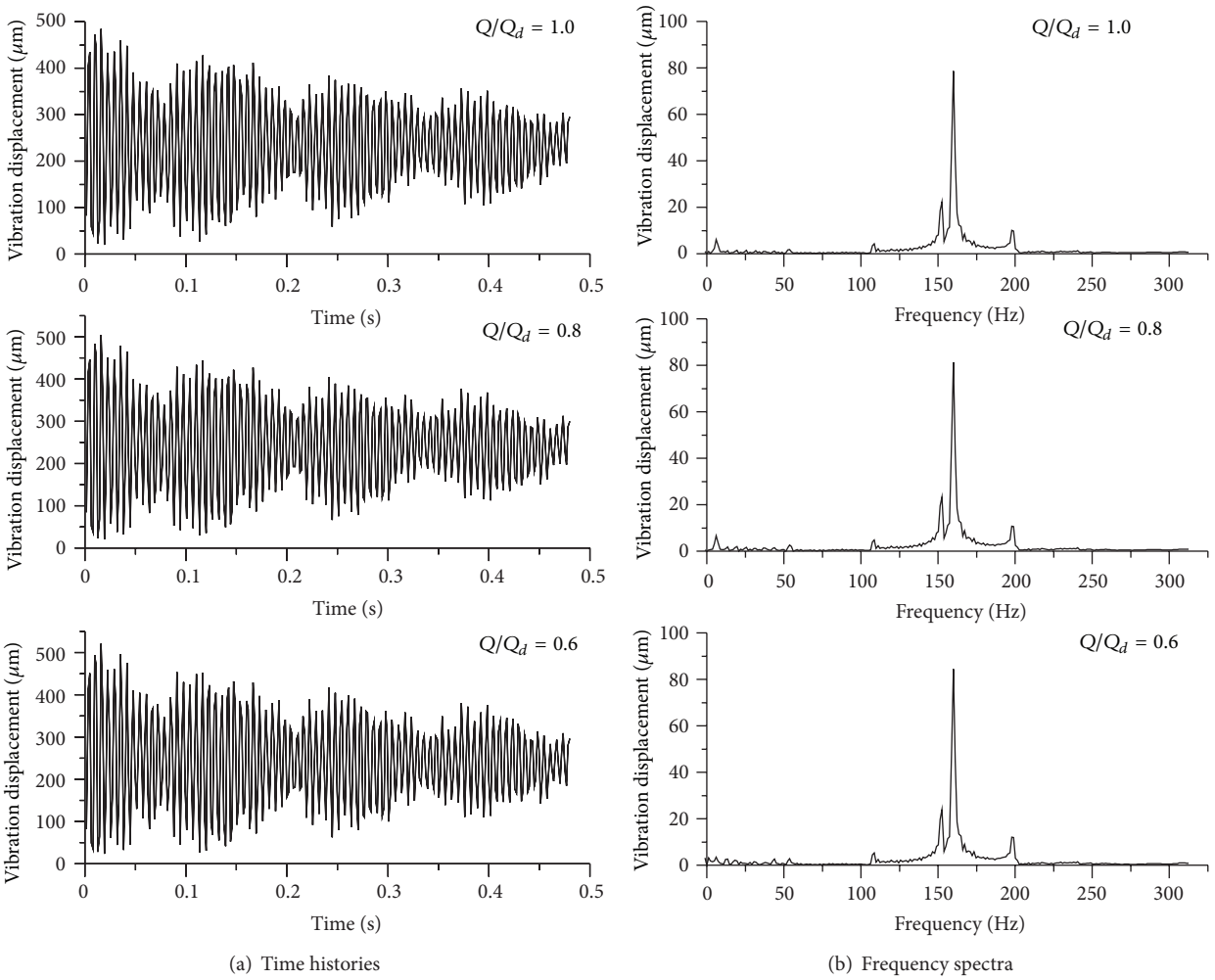

Figure 9: Vibration displacements at pump top point U5.

(2) At 0.6 Q_d, the maximum dynamic stress was 1.14 times that at Q_d, which was relatively lower than the difference in the corresponding pressure fluctuations, that is, 3.24 times. This revealed that dynamic stresses on the pump body were weakly in accordance with pressure fluctuations.

(3) Significant deformation can be mainly observed in four regions, namely, between the fourth to fifth hydraulic profiles, the sixth hydraulic profile of the volute casing, shaft bearing hole nearby, and the bottom of pump suction part close to the inlet nozzle. The maximum vibration displacement occurred close to the shaft bearing hole region, whereas comparable small displacements were detected at the inlet, outlet of pump, and the top region of the volute casing. The maximum amplitude was found to be around 7.5 times of the lowest one, for each operating condition. Moreover, the deformation at the pump outlet (U2) was slightly affected by flow rate variation, whereas the top region of the volute casing (U3) appeared quite sensitive.

Acknowledgments

This research is supported by the National Natural Science Foundation of China (no. 51139007) and the National Science & Technology Support Project of China (no. 2012BAD08B03).

References

[1] L. Y. Qi, R. Jiang, and J. J. Shi, "Research on type selection and operating scheme of large-scale pump unit with high head for Hui-nan-zhuang pump station," *South-to-North Water Transfers and Water Science and Technology*, vol. 6, no. 1, pp. 200–203, 2008.

[2] S. Chu, R. Dong, and J. Katz, "Relationship between unsteady flow, pressure fluctuations, and noise in a centrifugal pump—part A: use of PDV data to compute the pressure field," *Journal of Fluids Engineering*, vol. 117, no. 1, pp. 24–29, 1995.

[3] S. Chu, R. Dong, and J. Katz, "Relationship between unsteady flow, pressure fluctuations, and noise in a centrifugal pump—part B: effects of blade-tongue interactions," *Journal of Fluids Engineering*, vol. 117, no. 1, pp. 30–35, 1995.

[4] M. Toussaint, "Analysis of unsteady flow in centrifugal pump at off-design point operation," in *Proceedings of the 23rd IAHR Symposium on Hydraulic Machinery and Systems*, Paper no. F302, Yokohama, Japan, October 2006.

[5] Z. F. Yao, F. J. Wang, L. X. Qu, and R. F. Xiao, "Experimental investigation of time-frequency characteristics of pressure fluctuations in a double-suction centrifugal pump," *Journal of Fluids Engineering*, vol. 133, no. 10, Article ID 101303, 10 pages, 2011.

[6] J. González, J. M. F. Oro, and K. M. Argüelles-Díaz, "Flow analysis for a double suction centrifugal machine in the pump and turbine operation modes," *International Journal for Numerical Methods in Fluids*, vol. 61, no. 2, pp. 220–236, 2009.

[7] G. H. Cong and F. J. Wang, "Numerical investigation of unsteady pressure fluctuations near volute tongue in a double-suction centrifugal pump," *Transactions of the Chinese Society of Agricultural Machinery*, vol. 39, no. 6, pp. 60–67, 2008.

[8] L. X. Qu, F. J. Wang, G. H. Cong, and J. Y. Gao, "Effect of volute tongue-impeller gaps on the unsteady flow in double-suction centrifugal pump," *Transactions of the Chinese Society of Agricultural Machinery*, vol. 42, no. 7, pp. 50–55, 2011.

[9] L. X. Qu, F. J. Wang, G. H. Cong, and Z. F. Yao, "Pressure fluctuations of the impeller in a double-suction centrifugal pump," *Transactions of the Chinese Society of Agricultural Machinery*, vol. 42, no. 9, pp. 78–84, 2011.

[10] Z. J. Yang, *Large Eddy Simulation of 3D Flow in Centrifugal Pump*, China Agricultural University, Beijing, China, 2012.

[11] K. Kobayashi, S. Ono, I. Harada, and Y. Chiba, "Numerical analysis of stress on pump blade by one way coupled fluid structure simulation," *Journal of Fluid Science and Technology*, vol. 5, no. 2, pp. 219–234, 2010.

[12] L. X. Qu, F. J. Wang, Z. Q. Liu, and X. Y. Shi, "Numerical analysis of unsteady flow in a large double-suction centrifugal pump," in *Proceedings of the International Conference on Pumps and Fans*, Paper no. 049, Hangzhou, China, 2010.

[13] J. Y. Gao, F. J. Wang, L. X. Qu, Z. Q. Liu, and L. Y. Qi, "Dynamic stress of large double-suction centrifugal pump impeller," *Transactions of the Chinese Society of Agricultural Machinery*, vol. 43, no. 1, pp. 42–47, 2012.

[14] L. Y. He, F. J. Wang, J. Y. Gao, M. Yang, and L. X. Qu, "Modal analysis of double-suction centrifugal pump impellers," *Journal of Engineering Thermophysics*, vol. 32, no. 1, pp. 29–32, 2011.

[15] Y. Y. Jiang, S. Yoshimura, R. Imai, H. Katsura, T. Yoshida, and C. Kato, "Quantitative evaluation of flow-induced structural vibration and noise in turbomachinery by full-scale weakly coupled simulation," *Journal of Fluids and Structures*, vol. 23, no. 4, pp. 531–544, 2007.

[16] M. Yang, F. J. Wang, L. Y. Qi, and J. Y. Gao, "Fluid-structure coupling interface model and its application in dynamic analysis of hydraulic machinery," *Journal of Hydraulic Engineering*, vol. 42, no. 7, pp. 819–825, 2011.

[17] F. J. Wang, W. Zhao, M. Yang, and J. Y. Gao, "Analysis on unsteady fluid-structure interaction for a large scale hydraulic turbine II. Structure dynamic stress and fatigue reliability," *Journal of Hydraulic Engineering*, vol. 43, no. 1, pp. 15–21, 2012.

[18] X. C. Wang, *Finite Element Method*, Tsinghua University Press, Beijing, China, 2003.

[19] Z. F. Yao, F. J. Wang, R. F. Xiao, and C. L. He, "Experimental investigation of relationship between pressure fluctuations and vibrations for a double suction centrifugal pump," in *Proceedings of the ASME-JSME-KSME Joint Fluids Engineering Conference (AJK2011-FED)*, Hamamatsu, Japan, July 2011.